

A boosting approach for prostate cancer detection using multi-parametric MRI

Guillaume Lemaître^{a,b} and Joan Massich^a and Robert Martí^b and Jordi Freixenet^b and Joan C. Vilanova^c and Paul M. Walker^d and Désiré D. Sidibé^a and Fabrice Mériaudeau^a

^aLE2I-UMR CNRS 6306, Université de Bourgogne, 12 rue de la Fonderie, 71200 Le Creusot, France;

^bViCOROB, Universitat de Girona, Campus Montilivi, Edifici P4, 17071 Girona, Spain;

^cDepartment of Magnetic Resonance, Clinica Girona, Lorenzana 36, 17002 Girona, Spain

^dLE2I-UMR CNRS 6306, Université de Bourgogne, Avenue Alain Savary, 21000 Dijon, France;

ABSTRACT

Prostate cancer has been reported as the second most frequently diagnosed men cancers in the world. In the last decades, new imaging techniques based on MRI have been developed in order to improve the diagnosis task of radiologists. In practise, diagnosis can be affected by multiple factors reducing the chance to detect potential lesions. Computer-aided detection and computer-aided diagnosis have been designed to answer to these needs and provide help to radiologists in their daily duties. In this study, we proposed an automatic method to detect prostate cancer from a per voxel manner using 3T multi-parametric MRI and a gradient boosting classifier. The best performances are obtained using all multi-parametric information as well as zonal information. The sensitivity and specificity obtained are 86.9% and 84.6%, respectively.

Keywords: Gradient boosting, multi-parametric MRI, prostate cancer, computer-aided diagnosis

1. INTRODUCTION

On a worldwide scale, prostate cancer (PCa) has been reported as the second most frequently diagnosed men cancers accounting for 13.6%.¹ Statistically, the estimated number of new diagnosed cases was 899,000 with no less than 258,100 estimated deaths.¹ In United States, aside from skin cancer, PCa was declared to be the most commonly diagnosed cancer among men, implying that around one in seven men will be diagnosed with PCa during their lifetime.²

Since its introduction in mid-1980s, prostate-specific antigen (PSA) is widely used for PCa screening³ and has shown to improve early detection of PCa.⁴ However, several trials conducted in Europe and United States conclude that PSA screening suffers from low specificity.⁵⁻⁷ Thus, current research focus on developing new screening methods to improve PCa detection. In this perspective, Magnetic resonance imaging (MRI) techniques have recently shown promising results for PCa detection. Furthermore, three different modalities are currently investigated: (i) T₂ Weighted (T₂-W) MRI, (ii) Dynamic Contrast-Enhanced (DCE) MRI and (iii) Diffusion Weighted (DW) MRI.

Several researches have been carried out in order to investigate the contributions of machine learning classifiers for PCa detection using the three aforementioned 3T multi-parametric MRI such as Support Vector Machines (SVM),⁸⁻¹² probabilistic boosting tree¹³ or probabilistic neural network.¹³ However, these studies use different datasets and evaluation statistics to report their results. Thus, no fair comparisons between these different studies are possible.

In this research, we investigate the performance of gradient boosting for PCa detection using 3T multi-parametric MRI. Two different features extraction strategies have been chosen in order to feed the classifier: (i) voxel-based and (ii) 3D texton-based. An evaluation of both strategies as well as the contribution of each modality is provided. Furthermore, the dataset used for this experimentation is part of our future benchmarking platform I2CVB available at <http://visor.udg.edu/i2cvb/> and are ready for future comparisons.

Further author information: (Send correspondence to G.L.)

G.L.: E-mail: guillaume.lemaitre@udg.edu

2. MATERIAL AND METHODS

2.1 Data

The multi-parametric MRI was acquired from a cohort of patients with higher-than-normal level of PSA. The acquisition was performed using a 3T whole body MRI scanner (Siemens Magnetom Trio TIM, Erlangen, Germany) using sequences to obtain T₂-W MRI, DCE MRI and DW MRI. Aside of the MRI examination, these patients also underwent a guided-biopsy. Finally, the dataset was composed of a total of 20 patients of which 18 patients had biopsy proven PCa and 2 patients were “healthy” with negative biopsies. The prostate organ as well as the prostate zones (i.e., peripheral zone (PZ) and central gland (CG)) and PCa were manually segmented by an experienced radiologist. Therefore, 13 patients had a PCa in the PZ, 3 patients had PCa in the CG, 2 patients had invasive PCa in both PZ and CG and finally 2 patients were considered as “healthy”.

The Apparent Diffusion Coefficient (ADC) maps were computed using the scanner software and the DW MRI. The DCE MRI sequence consist in a kinetic study composed of 40 samples over time. These DCE MRI sequences and ADC maps were resampled using the spatial information of the T₂-W MRI sequence with dimensions of $448 \times 360 \times 64$ and voxel spacing of $0.68 \times 0.68 \times 1.25$ mm³. Linear interpolation was used to compute missing data during the up-sampling. The resampling was implemented in C++ using the Insight Segmentation and Registration Toolkit.¹⁴

Due to the large number of samples available at a voxel scale, the dataset was pre-processed in order to deal with a balanced dataset allowing to not bias the results. Therefore, all the positive samples (i.e., PCa voxels) were stored and an equal number of negative samples (i.e., “healthy” voxels) were randomly selected from the larger original pool. Thus, the total amount of positive and negative samples considered in our experiments accounted for 218,422 voxels.

2.2 Classification framework

2.2.1 Feature extraction strategies

Table 1: Overview of voxel features extracted in our classification framework.

Extraction strategy	Name	Size	Short description
Voxel-based	v_{T_2-W}	1	Intensity of a voxel in the T ₂ -W MRI
	V_{ADC}	1	Intensity of a voxel in the ADC map
	V_{DCE}	40	Intensities of a voxel along the whole serie in the DCE MRI
	V_{PZ}	1	Boolean value of a voxel membership to the PZ
	V_{CG}	1	Boolean value of a voxel membership to the CG
3D texton-based	T_{T_2-W}	243	Intensities vector for a window of $9 \times 9 \times 3$ voxels in the T ₂ -W MRI
	T_{ADC}	243	Intensities vector for a window of $9 \times 9 \times 3$ voxels in the ADC map
	T_{DCE}	9720	Intensities vector for a window of $9 \times 9 \times 3$ along the whole serie in the DCE MRI
	T_{PZ}	243	Boolean vector of voxels memberships to the PZ for a window of $9 \times 9 \times 3$
	T_{CG}	243	Boolean vector of voxels memberships to the CG for a window of $9 \times 9 \times 3$

A summary of the extracted features as well as the chosen strategies are summarized in Table 1. Two main strategies are applied to extract features. In the voxel-based approach, at each voxel location, the intensities for

the different MRI modalities are extracted as well as the membership of this voxel to belong to the PZ or CG. The 3D texton-based approach extend this extraction for a 3D window of size $9 \times 9 \times 3$ around the central voxel. In both case, the vectors $V(\cdot)$ and $T(\cdot)$ extracted are scaled using min-max normalization.

Table 2: Overview of the different combinations of features tested for the classification.

Voxel-based	V_{T_2-W}	V_{ADC}	V_{DCE}	V_{PZ}	V_{CG}	Texton-based	T_{T_2-W}	T_{ADC}	T_{DCE}	T_{PZ}	T_{CG}
V_1	✓	✗	✗	✗	✗	T_1	✓	✗	✗	✗	✗
V_2	✗	✓	✗	✗	✗	T_2	✗	✓	✗	✗	✗
V_3	✗	✗	✓	✗	✗	T_3	✗	✗	✓	✗	✗
V_4	✓	✓	✗	✗	✗	T_4	✓	✓	✗	✗	✗
V_5	✓	✗	✓	✗	✗	T_5	✓	✗	✓	✗	✗
V_6	✗	✓	✓	✗	✗	T_6	✗	✓	✓	✗	✗
V_7	✓	✓	✓	✗	✗	T_7	✓	✓	✓	✗	✗
V_8	✓	✓	✓	✓	✓	T_8	✓	✓	✓	✓	✓

Then, the different concatenation of the vectors $V(\cdot)$ and $T(\cdot)$ are summarized in Table 2. Different combinations are further tested in order to observe the contribution of each data feature.

2.2.2 Gradient boosting

In this research, a gradient boosting classifier¹⁵ originally proposed by Friedman^{16,17} is used for the implementation of our computer-aided detection and diagnosis (CAD) system for PCa. Gradient boosting is in fact a reformulation of the well-known AdaBoost¹⁸ in which the problem of finding “boots” is tackled as a numerical optimization. In a greedy manner, a strong classifier is constructed by iteratively finding the best pair of real-valued weak learner function (e.g., regression trees) and its corresponding weight which minimizes a given differentiable loss function. This minimization can be carried out via gradient descent or quadratic approximation.¹⁹

In this work, the weak learner function used is the regression trees while the loss function is an exponential loss.

2.2.3 Validation model

All the different combinations reported in Table 2 were classified using a ten-fold cross-validation procedure, of which nine-fold were used as training samples and one-fold was kept as testing samples and the experiments were repeated for ten iterations.

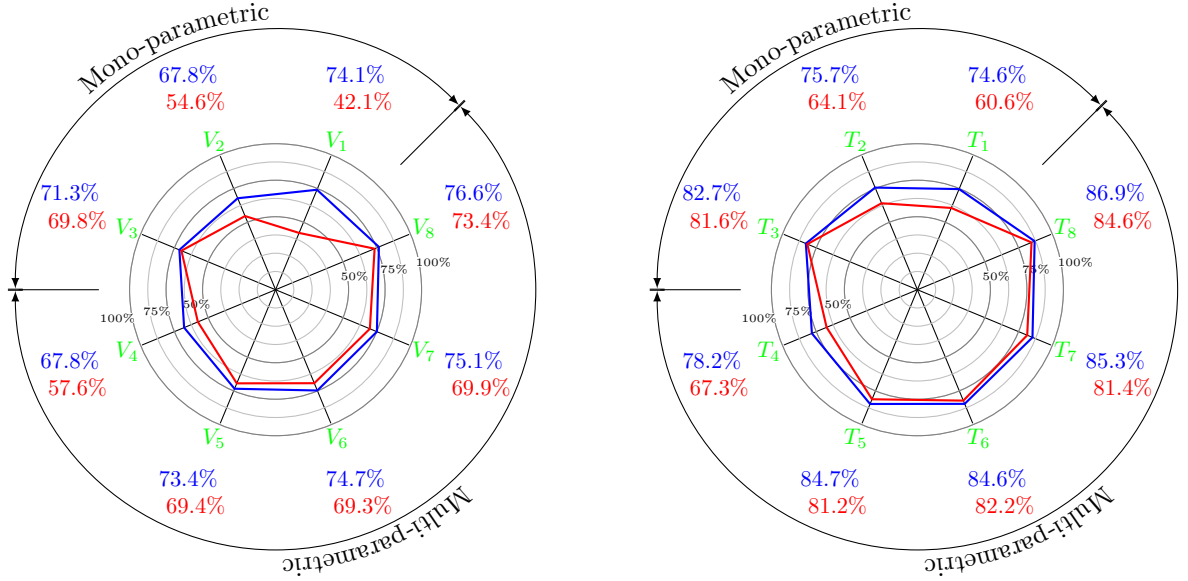
3. RESULTS AND DISCUSSION

The classification results obtained are depicted in Fig. 1. The best classification performances are achieved using the 3D texton-based extraction strategy and a combination of the three different modalities and the zonal information. The sensitivity and specificity obtained are 86.9% and 84.6%, respectively.

Analyzing the classification outcomes of each single modality, the ADC map is the most discriminative feature with superior performances than the combination of T_2 -W MRI and DCE MRI together. However, the two latter mentioned modalities provide relevant information since that the combination of the three of them enhances the reported sensitivity and specificity.

Integrating information about the prostate zones (i.e., PZ and CG) boosts the classification performances. More precisely, this feature allows to improve greatly the specificity and slightly the sensitivity.

In overall, the 3D texton-based strategy leads to better classification while results compared with the voxel-based strategy for all the mono and multi parametric combinations experimented. Thus, integrating spatial information about the neighborhood of a given voxel should lead to drastic improvements.



(a) Voxel-based features

(b) 3D texton-based features

Figure 1: Comparison between the combination of features introduced in Table 2 in terms of sensitivity and specificity are illustrated in blue and red, respectively.

4. CONCLUSION

In this study, an exhaustive analysis of classification of 3T multi-parametric MRI data using a gradient boosting classifier has been carried out. The best classification performances are obtained by extracting the features using a 3D texton-based strategy and using the information from all the modalities as well as the zonal information. A maximum sensitivity and specificity of 86.9% and 84.6% respectively, are reached.

Two avenues for future research can be explored. First, the registration of the multi-parametric data has been discarded and could be performed ahead of the classification to study the possible improvements implied. Then, other features than intensities could be extracted and the results could be compared with the described experiments here, since that the dataset used is public.

ACKNOWLEDGMENTS

Guillaume Lemaître was supported by the Generalitat de Catalunya (grant nb. FI-DGR2012) and partly by the Mediterranean Office for Youth (grant nb. 2011/018/06). We would like also to thank the Clinica Girona (Catalunya, Espanya) and the Centre Hospitalier of Dijon (France) for providing the MRI images used in this research.

BIOGRAPHY

Guillaume Lemaître received an Erasmus Mundus MSc in Vision and Robotic (ViBOT) from the Heriot-Watt University, Université de Bourgogne and Universitat de Girona as well as a MSc in Business Innovation and Technology Management (BITM) from the Universitat de Girona. He is currently carrying out a joint PhD at the Université de Bourgogne and Universitat de Girona focusing on the development of computer-aided diagnosis for prostate cancer.

REFERENCES

1. J. Ferlay, H. R. Shin, F. Bray, D. Forman, C. Mathers, and D. M. Parkin, “Estimates of worldwide burden of cancer in 2008: GLOBOCAN 2008,” *Int. J. Cancer* **127**, pp. 2893–2917, Dec 2010.

2. R. Siegel, J. Ma, Z. Zou, and A. Jemal, "Cancer statistics, 2014," *CA: A Cancer Journal for Clinicians* **64**(1), pp. 9–29, 2014.
3. R. Etzioni, D. F. Penson, J. M. Legler, D. di Tommaso, R. Boer, P. H. Gann, and E. J. Feuer, "Overdiagnosis due to prostate-specific antigen screening: lessons from U.S. prostate cancer incidence trends," *J. Natl. Cancer Inst.* **94**, pp. 981–990, Jul 2002.
4. R. Chou, J. M. Croswell, T. Dana, C. Bougatsos, I. Blazina, R. Fu, K. Gleitsmann, H. C. Koenig, C. Lam, A. Maltz, J. B. Ruge, and K. Lin, "Screening for prostate cancer: a review of the evidence for the U.S. Preventive Services Task Force," *Ann. Intern. Med.* **155**, pp. 762–771, Dec 2011.
5. G. L. Andriole, E. D. Crawford, R. L. Grubb, S. S. Buys, D. Chia, T. R. Church, M. N. Fouad, E. P. Gelmann, P. A. Kvale, D. J. Reding, J. L. Weissfeld, L. A. Yokochi, B. O'Brien, J. D. Clapp, J. M. Rathmell, T. L. Riley, R. B. Hayes, B. S. Kramer, G. Izmirlian, A. B. Miller, P. F. Pinsky, P. C. Prorok, J. K. Gohagan, and C. D. Berg, "Mortality results from a randomized Prostate-cancer screening trial," *New England Journal of Medicine* **360**(13), pp. 1310–1319, 2009.
6. J. Hugosson, S. Carlsson, G. Aus, S. Bergdahl, A. Khatami, P. Lodding, C. G. Pihl, J. Stranne, E. Holmberg, and H. Lilja, "Mortality results from the Göteborg randomised population-based prostate-cancer screening trial," *Lancet Oncol.* **11**, pp. 725–732, Aug 2010.
7. F. H. Schröder, J. Hugosson, M. J. Roobol, T. L. Tammela, S. Ciatto, V. Nelen, M. Kwiatkowski, M. Lujan, H. Lilja, M. Zappa, L. J. Denis, F. Recker, A. Pez, L. Määtänen, C. H. Bangma, G. Aus, S. Carlsson, A. Villers, X. Rebillard, T. van der Kwast, P. M. Kujala, B. G. Blijenberg, U.-H. Stenman, A. Huber, K. Taari, M. Hakama, S. M. Moss, H. J. de Koning, and A. Auvinen, "Prostate-cancer mortality at 11 years of follow-up," *New England Journal of Medicine* **366**(11), pp. 981–990, 2012.
8. G. J. S. Litjens, P. C. Vos, J. O. Barentsz, N. Karssemeijer, and H. J. Huisman, "Automatic computer aided detection of abnormalities in multi-parametric prostate MRI," in *Proc. SPIE 7963, Medical Imaging 2011: Computer-Aided Diagnosis*, pp. 79630T–79630T–7, 2011.
9. G. Litjens, O. Debats, W. van de Ven, N. Karssemeijer, and H. Huisman, "A pattern recognition approach to zonal segmentation of the prostate on MRI," *Med Image Comput Comput Assist Interv* **15**(Pt 2), pp. 413–420, 2012.
10. G. Litjens, O. Debats, J. Barentsz, N. Karssemeijer, and H. Huisman, "Computer-aided detection of prostate cancer in MRI," *Medical Imaging, IEEE Transactions on* **33**, pp. 1083–1092, May 2014.
11. P. Liu, S. Wang, B. Turkbey, P. C. P. Grant, K. and Pinto, B. J. Wood, and R. M. Summers, "A prostate cancer computer-aided diagnosis system using multimodal magnetic resonance imaging and targeted biopsy labels," in *Proc. SPIE 8670, Medical Imaging 2013: Computer-Aided Diagnosis*, pp. 86701G–86701G–6, 2013.
12. Y. Peng, Y. Jiang, C. Yang, J. Brown, T. Antic, I. Sethi, C. Schmid-Tannwald, M. Giger, S. Eggener, and A. Oto, "Quantitative analysis of multiparametric prostate MR images: differentiation between prostate cancer and normal tissue and correlation with Gleason score—a computer-aided diagnosis development study," *Radiology* **267**, pp. 787–796, June 2013.
13. S. Viswanath, B. N. Bloch, J. Chappelow, P. Patel, N. Rofsky, R. Lenkinski, E. Genega, and A. Madabhushi, "Enhanced multi-protocol analysis via intelligent supervised embedding (EMPrAvISE): detecting prostate cancer on multi-parametric MRI," in *Proc. SPIE 7963, Medical Imaging 2011: Computer-Aided Diagnosis*, 2011.
14. H. J. Johnson, M. McCormick, L. Ibáñez, and T. I. S. Consortium, *The ITK Software Guide*. Kitware, Inc., third ed., 2013. *In press*.
15. C. Becker, R. Rigamonti, V. Lepetit, and P. Fua, "Supervised feature learning for curvilinear structure segmentation," in *Medical Image Computing and Computer-Assisted Intervention MICCAI 2013*, K. Mori, I. Sakuma, Y. Sato, C. Barillot, and N. Navab, eds., *Lecture Notes in Computer Science* **8149**, pp. 526–533, Springer Berlin Heidelberg, 2013.
16. J. H. Friedman, "Stochastic Gradient Boosting," *Computational Statistics and Data Analysis* **38**, pp. 367–378, 1999.
17. J. H. Friedman, "Greedy Function Approximation: A Gradient Boosting Machine," *Annals of Statistics* **29**, pp. 1189–1232, 2000.

18. Y. Freund and R. Schapire, “A decision-theoretic generalization of on-line learning and an application to boosting,” *Journal of Computer and System Sciences* **55**(1), pp. 119 – 139, 1997.
19. Z. Zheng, H. Zha, T. Zhang, O. Chapelle, K. Chen, and G. Sun, “A general boosting method and its application to learning ranking functions for web search neur,” in *Inf. Proc. Sys. Conf*, pp. 1697–1704, 2008.